Journal Name

ARTICLE TYPE

Cite this: DOI: 10.1039/xxxxxxxxxx

From quantum fragments to Lewis structures: electron counting in position space†

A. Martín Pendás*, E. Francisco

Received Date
Accepted Date

DOI: 10.1039/xxxxxxxxxx

www.rsc.org/journalname

An electron counting technique that easily provides Lewis structures from real space analyses of general wavefunctions is proposed. We base our approach on reformulating the adaptive natural density partitioning (AdNDP) algorithm proposed by Zubarev and Boldyrev (*Phys. Chem. Chem. Phys.* **10**, 5207 (2008)) in position space through the use of domain-averaged cumulant densities, which take into account many-electron correlations. Averages are performed over the basins provided by the quantum theory of atoms in molecules. The decomposition gives rise to a set of n-center, two-electron orbitals which describe the dominant Lewis structures of a molecular system, and is available both for single- and multi-determinant wavefunctions. As shown through several examples, chemically intuitive Lewis descriptions are now available from fully orbital invariant position space descriptors. In this sense, real space methods are now in a position to compete with natural bond order (NBO) orbital procedures without the many biases of the latter.

Introduction

The two-center two-electron (2c,2e) bond is, still today, the basic buiding block in the accepted theory of chemical bonding. Proposed about a hundred years ago,[1] it has resisted well the unavoidable aging process of any evolving paradigm. Actually, grouping electrons in pairs, be them of the core, lone or bonding types, has become inherent to chemistry as a science. In the meantime, theoretical chemists have argued for a long time about how to recover the Lewis pair from the underlying quantum mechanical framework.[2] This is relatively simple in the mean-field approximation, where populating opposite spin one-electron states in an independent way leads to the doubly occupied orbitals. The compatibility of this molecular orbital (MO) picture,[3] which generally provides delocalized states, with standard chemical concepts may be achieved via a plethora of orbital localization procedures.[4–14] The enterprise is far less obvious in the case of correlated descriptions, although the revitalization of valence bond (VB) theory in recent times[15–20] yields chemical pictures easier to couple with the chemist's localized perception of Lewis pairs.

Localization procedures may fail to provide consistent chemical descriptions within the orthodox Lewis picture whenever multiple resonance structures are needed, e.g. when aromaticity sets in, or when pairs delocalize over more than two atoms. This gives rise to multi-center bonding, a concept of historical interest that, for instance, was basic to rationalize the structure and chemistry of boron compounds.[21] This extended Lewis framework, in which a set of resonance structures made up from n-center two-electron bonds (nc,2e) are used to model the electronic structure of a molecule, has become a *de facto* standard in the theory of the chemical bond. From a computational point of view, one of its best known implementations is the natural bond orbital (NBO) analysis of Weinhold and coworkers,[22–25] together with its associated donor-acceptor paradigm.

In brief, the NBO procedure provides a generalization of Löwdin's natural orbitals, i.e. the eigenvectors of the first order reduced density matrix (1RDM) characterized by displaying maximal electron occupancies. The procedure works by successively diagonalizing atomic, di-atomic or generally n-center blocks of the 1RDM. This is done in Fock space, usually in a localized basis set, so a first worry is to obtain an appropriate minimal occupied atomic basis together with its unoccupied complement: the natural atomic orbital (NAO) basis. In order to obtain objects as independent of the basis set as possible, as well as to avoid other more subtle problems, the NAO/NBO algorithm is considerably more cumbersome than this simplified description, involving several somewhat controversial decisions.[26] Although NBOs may be obtained from correlated 1RDMs, a reconstruction of the system's wavefunction can only be made easily in the case of a single-determinant. It is also interesting to notice that the NBO scheme has traditionally not been applied beyond the 3-center case, al-

Departamento de Química Física y Analítica, Universidad de Oviedo, Oviedo. Spain. E-mail: ampendas@uniovi.es

† Electronic Supplementary Information (ESI) available: See DOI: 10.1039/b000000x/

though the most recent versions of the code allow for extensions up to a number of centers equal to nine.

A simpler generalization of the NBO apparatus to the true many-center situation was provided by Zubarev and Boldyrev,[27] through their adaptive natural density partitioning (AdNDP). In AdNDP, the n-center blocks of the 1RDM are diagonalized after depleting them from the eigenvectors with large (≈ 2) occupancies obtained in the $(n-1)$-center step of an iterative process. In this way, cores and lone pairs are obtained first, then eliminated from the 1RDM before obtaining (2c,2e) bonds, etc. The procedure is fast and easy to implement. It has also been applied to periodic systems, and provides a standard Lewis description in simple cases as well as appealing images of electron delocalization in more complex ones, such as metallic clusters.[28–32]

Despite their clear success, both NBO and AdNDP heavily rest on prescriptions which are not invariant under orbital transformations. There exists, however, a whole discipline in the theory of the chemical bond that advocates for the use of orbital invariant descriptors based on RDMs. These RDMs may be written either in momentum or position space, the latter being more interesting to Chemistry. Position space techniques have been quite successful[33] in the past, providing important insights into chemical bonding problems without recourse to orbitals. In many of these approaches, a control scalar field, such as the electron density, ρ, or the electron localization function (ELF),[34] is used to define a topology and an exhaustive partition of the physical space R^3 into chemical regions. This leads to a direct and orbital invariant association of points in space to, for instance, atoms, like it is done in the quantum theory of atoms in molecules (QTAIM) if the control scalar field is ρ.[35] A rather insightful energy decomposition analysis, the interacting quantum atoms (IQA) approach,[36,37] has also been devised according to these ideas.

Nevertheless, powerful as it is, position space reasoning lacks a direct link to the Lewis model, and without orbitals (or effective one-electron functions), its penetration in the non-theoretical chemistry community is, to say the least, difficult. As we have stressed before,[38] the theoretical or computational constructs that have spread most quickly in the literature (like the NBO technique) are those closer to the Lewis-like mind of Chemistry practitioners. Recovering effective one-electron functions from orbital invariant position space theories is thus a worthwhile enterprise.

We have recently shown that a full hierarchy of one-electron functions describing n-center bonding, the natural adaptive orbitals (NAdOs),[38,39] can be obtained from the domain-averaged $(n+1)-$th order cumulant density (CD).[40] The $n-$th order CD (nCD) is simply the diagonal part of the standard $n-$th order RDM that can not be expressed in terms of lower order RDMs.[41] Since we do not focus here on technicalities but rather on the usefulness of the approach to Chemistry, we avoid details and nitty-gritties. Explicit formulas for CDs can be found elsewhere,[39] and more details on the construction and physical meaning of the NAdOs of a general order are given in the Supplementary Information.

For the time being, it is only necessary to consider the second order CD, that coincides with the exchange-correlation density, $\rho_c^2(\boldsymbol{r}_1,\boldsymbol{r}_2) = \rho(\boldsymbol{r}_1)\rho(\boldsymbol{r}_2) - \rho^2(\boldsymbol{r}_1,\boldsymbol{r}_2)$, where $\rho^2(\boldsymbol{r}_1,\boldsymbol{r}_2)$ is the diagonal 2RDM. The exchange-correlation density measures deviation of the pair density from that of independent particles. If a division of the physical space, R^3, into atomic regions is performed, $R^3 = \bigcup_{a=1}^{m} \Omega_a$, and the $\boldsymbol{r}_2$ coordinate of $\rho_c^2(\boldsymbol{r}_1,\boldsymbol{r}_2)$ is averaged over the Ω_a's, the following decomposition of $\rho(\boldsymbol{r})$ appears[38]

$$\rho(\boldsymbol{r}) \quad = \quad \sum_a^m \rho^a(\boldsymbol{r}) = \sum_a^m \int_{\Omega_a} d\boldsymbol{r}_2 \rho_c^2(\boldsymbol{r},\boldsymbol{r}_2). \tag{1}$$

This can equally be done with the full 2RDM, leading to a decomposition of $\rho(\boldsymbol{r},\boldsymbol{r}')$ into atomic $\rho^a(\boldsymbol{r};\boldsymbol{r}')$ components that can be diagonalized (usually by expressing them in an orbital basis. Doing so, we may write

$$\rho^a(\boldsymbol{r}) = \sum_i n_i^a \left[\phi_i^a(\boldsymbol{r})\right]^2, \tag{2}$$

where the $\phi_i^a(\boldsymbol{r})$'s and n_i^a's are the 1-center NAdOs and their occupations, respectively. These ϕ_i^a's coincide with the domain natural orbitals (DNOs) introduced by Ponec in the nineties.[42,43] They contain information about electron delocalization and are self-localizing entities, with occupations that add to the average electron population of the domain (e.g. atom). The closer to 2.0 n_i^a is, the more localized ϕ_i^a is in Ω_a. If n_i^a is clearly different from 2.0, the DNO leaks out of the domain, denoting bonding to other centers. This links, as expected, bonding with delocalization. At the Hartree-Fock level the occupations have been shown to be directly connected to the statistics of the electron populations of the domains, and also to their participation in the bond order (delocalization index, DI) of the domain with the rest of the system.[44,45] It has also been shown that, at this level, exact Lewis pairs between the domain and its complement can be recovered. This correspondence ceases to be exact for the correlated case, although in many cases a good match between DNOs and pairs can still be obtained.[45,46]

We use in this work the above ideas, combined with the NBO/AdNDP formalisms, to show how a generalized Lewis picture constructed from n-center two-electron functions can be easily built within the NAdOs hierarchy. With this, we intend to approach position space techniques to a general chemistry audience. Since the new protocol is consistent (i.e. compatible) with the underlying QTAIM analyses, all n-center NAdOs, bond indices, domain observables or IQA decompositions obtained from a given molecular wavefunction refer to the same grand image. In this sense, we believe that real space methods are now in a position to compete with NBO-like orbital procedures. They offer simultaneously a generalized population analysis that includes multi-center bond indices, rules to build Lewis structures, energy decomposition analyses, and a large number of other by-products.

We have divided the rest of the article as follows. First, our method to recover the Lewis structures through a real space adaptive natural cumulant partitioning (rs-AdNCP) is described. Then we illustrate the ability of this new method to describe some diatomic and simple polyatomic molecules, the multicenter bonding of some boron compounds, and the bonding patterns of some exotic sytems. Finally, the main conclusions of this work are summarized.

Real space adaptive natural cumulant partitioning (rs-AdNCP)

The adaptive natural density partitioning (AdNDP) as defined by Zubarev and Boldyrev,[27] is based on successively diagonalizing the n-atomic blocks of the 1RDM written in the natural atomic orbital (NAO) basis of Weinberg and coworkers. In this basis, each element $P_{\mu\nu}$ of the 1RDM has an atomic label associated to each of its row and column indices. Ordering the basis functions atomic-wise, we denote $\boldsymbol{P}_{ij}$ as the block formed by row and column indices belonging to atom i and j, respectively. Diagonalization of the $\boldsymbol{P}_{ii}$ block (taking care of non-orthogonality this leads to solving $\boldsymbol{P}_{ii}\phi^i_\lambda = n^i_\lambda \boldsymbol{S}_{ii}\phi^i_\lambda$) provides a set of eigenfunctions ϕ^i_λ. Those with occupations close to 2 are considered cores or lone pairs of center i, and stored. The full density matrix is then depleted from the stored vectors, $\boldsymbol{P} \leftarrow \boldsymbol{P} - \sum_\lambda^{\text{stored}} n^i_\lambda \boldsymbol{\phi}^{i\dagger}_\lambda \boldsymbol{\phi}^i_\lambda$. After the one-center step has run over all centers, the two-center 2×2 blocks are constructed from the depleted matrix,

$$\boldsymbol{P}^{(ij)} = \begin{pmatrix} \boldsymbol{P}_{ii} & \boldsymbol{P}_{ij} \\ \boldsymbol{P}_{ji} & \boldsymbol{P}_{jj} \end{pmatrix}, \tag{3}$$

and diagonalized. Highly occupied eigenvectors, $\phi^{(ij)}_\lambda$, interpreted as (2c,2e) bonds, are again stored and depleted from the full density, and the process is repeated with 3×3, and further order blocks until the total number of electrons has been recovered to a given precision. This provides a generalized Lewis description of the system in terms of a set of (nc,2e) bonds. The AdNDP recipe is simple, efficient, and leads to very robust results. Orbitals from different diagonalizations are not orthogonal, but can be orthogonalized with no big loss of information, if needed.

These ideas are immediately generalizable in real space. We will explain our strategy starting with Eqs. 1 and 2, where a is an atom of the system. As we have said in the Introduction, DNOs ϕ^a_i with occupations n^a_i close to 2 are highly localized in their atomic domains, representing either cores or lone pairs. Similarly, if we construct a quantum domain formed by the union of two atomic ones, $\Omega_{ab} = \Omega_a \bigcup \Omega_b$, the eigenvectors ($\phi^{ab}_i$) of $\rho^{ab} \equiv \rho^a + \rho^b$ with occupation numbers (n^{ab}_i) close to 2 will again be highly localized in the $\Omega_{ab} = \Omega_a + \Omega_b$ domain, containing also (2c,2e) solutions. If prior to the diagonalization of ρ^{ab} we deplete it from the Ω_a and Ω_b highly occupied vectors, only the (2c,2e) solutions will remain as eigenvectors with high population. This can be iterated to n centers.

The algorithm works as follows. In a first step, the ρ^a matrices for all the atomic domains ($a = 1,\ldots,m$) are obtained from the 2CD (Eq. 1). These are usually written in terms of the underlying canonical, fixed orbital basis, $\boldsymbol{\varphi}$: $\rho^a(\boldsymbol{r};\boldsymbol{r}') = \boldsymbol{\varphi}^\dagger(\boldsymbol{r}')\boldsymbol{G}^a\boldsymbol{\varphi}(\boldsymbol{r})$. Each $\boldsymbol{G}^a$ is then diagonalized, its eigenvectors $\boldsymbol{\phi}^a_\lambda$ with high occupations ($n^a_\lambda \approx 2$, a threshold value is chosen) selected and stored. After all centers have been considered, in a second step, the $\boldsymbol{G}^{ab} = \boldsymbol{G}^a + \boldsymbol{G}^b$ matrices are constructed for ab pairs, and the set of all previously found highly occupied eigenvectors (expressed back in the canonical basis) subtracted from them,

$$\tilde{\boldsymbol{G}}^{ab} = \boldsymbol{G}^{ab} - \sum_\lambda^{\text{stored}} n^a_\lambda \boldsymbol{\phi}^{a\dagger}_\lambda \boldsymbol{\phi}^a_\lambda. \tag{4}$$

Notice that since the basis is common, the $\boldsymbol{G}^{ab}$ matrix is not obtained through a selection of blocks as in the standard AdNDP approach, but by a simple matrix addition. Now, the $\tilde{\boldsymbol{G}}^{ab}$'s are diagonalized to find (2c,2e) bonds, which are again stored. The procedure is then repeated by constructing the $\boldsymbol{G}^{abc} = \boldsymbol{G}^a + \boldsymbol{G}^b + \boldsymbol{G}^c$ matrices for abc trios, which we deplete from all the one- and two-center stored functions, i.e.,

$$\tilde{\boldsymbol{G}}^{abc} = \boldsymbol{G}^{abc} - \sum_\lambda^{\text{stored}} n^a_\lambda \boldsymbol{\phi}^{a\dagger}_\lambda \boldsymbol{\phi}^a_\lambda - \sum_\lambda^{\text{stored}} n^{ab}_\lambda \boldsymbol{\phi}^{ab\dagger}_\lambda \boldsymbol{\phi}^{ab}_\lambda, \tag{5}$$

etc, until the total number of electrons has been exhausted. As in AdNDP, a generalized Lewis structure is obtained.

This rs-AdNCP procedure can be speeded up in several ways. First, hydrogen atoms can be skipped if desired in the first step, since it is highly unlikely that any of the n^{H}_λ's will be very close to 2.0, unless any of the H atoms have a net charge close to -1.[44] Second, the connectivity matrix of the molecule can be obtained prior to the rs-AdNCP analysis (using, for instance, a pure geometrical recipe based of the covalent radii of the atoms)[47] and the construction of the $\tilde{\boldsymbol{G}}^{ab}$'s then restricted to those pairs separated by no more than n_b *links* (say, $n_b \sim 2-4$). Finally, when the total number of electrons is not exhausted through the previous one and two center diagonalizations, a considerable number of sterile three- and further order diagonalizacions (i.e., not providing eigenvectors with occupations close to 2) can be avoided by carefully selecting the trios, quartets, ... n-tuples of atoms to be analyzed. For instance, by considering only sets of atoms in which each of the atoms is connected to at least one of the remaining ones in the set.

The rs-AdNCP prescription just described differs in an essential way from Fock-based AdNDPs. The first order matrix $\boldsymbol{P}$ used in AdNDP contains information about electron correlation in an effective way, at most. On the contrary, the ρ^a components from which the present decomposition is built upon inform about how the Fermi (actually the full exchange-correlation) hole is delocalized. They thus contain explicit correlation information. As it is known, the first order density is not much affected by electron correlation, while the exchange-correlation density can be qualitatively different in strongly correlated regimes. We thus expect that the decomposition presented in this work may show relevant differences with respect to NBO/AdNDP in interesting cases. Although we simply present here the rs-AdNCP machinery and apply it to a few examples, a system in which such a discrepancy is observed is the B_5^- anion, see below. Further work needs of course to be done to explore other possibly conflicting cases. It should also be stated that AdNDP needs not coincide with rs-AdNCP in every case. Although we have found no counterexamples up to now, we expect them when topological atomic populations differ considerably from NBO ones.

Although we have decided, for the sake of clarity, to consider

a spinless version of rs-AdNCP, the algorithms can immediately be generalized to the spin-resolved case. This is advantageous in the case of open-shell systems, which can be treated either via spin-resolved or spinless cumulants. Spin-resolved solutions offer a simple way to rationalize (nc,me) bonds where m is an odd number. A simple example will be shown below.

Recovering generalized Lewis structures in real space through rs-AdNCP

We devote this Section to showing the outcome of the rs-AdNCP procedure as applied to domain-averaged 2CDs. We have thus integrated the exchange-correlation density over QTAIM atomic domains both for single-determinant and correlated cases. The ρ^a matrices, expressed in the canonical MO basis, have been then subjected to the position space iterative diagonalization procedure as explained. Global density matrices were obtained with the GAMESS[48] (at the HF and DFT levels) and the PySCF[49] (at the explicitly correlated levels) suites, that feed the PROMOLDEN[50] and EDF[51] codes which provide the QTAIM atomic basins and the final rs-ADNCP functions, respectively.

Diatomics

Diatomics are particularly simple, yet instructive systems in which to examine the results obtained. First we recall that if a system is comprised by just two atoms a and b, then $\rho^a+\rho^b\equiv\rho^{ab}=\rho$, so diagonalizing the two-center contributions without depleting them from one-center functions will simply provide the usual natural orbital decomposition, with occupations equal to the natural orbital occupations. At the single-determinant level, they would simply be the canonical orbitals. This indicates the power of the approach.

Let us take the Be_2 and C_2 molecules as two simple examples, calculated at the NIST[52] geometries with the cc-pVDZ basis set. At the HF level, diagonalization of ρ^a provides a single core with eigenvalue almost equal to 2.0 and a remaining set of functions with smaller eigenvalues that delocalize, more or less, over the other center. If the threshold for accepting one-center functions is set to our default value $\varepsilon=1.90$, the rest of the electrons in both systems, $N-4$, are obtained in the two-center step after depleting $\rho^a+\rho^b=\rho$ from the cores. These two-center functions ϕ^{ab} are almost canonical orbitals. Two, of σ_g and σ_u symmetries, in Be_2, and four, adding a pair of functions $(\pi_{g,x},\pi_{g,y})$ to the former, in C_2.

These two molecules show two common problems of standard Lewis structures: how to deal with weak bonds, like in Be_2, and how to distinguish not strictly pure lone pairs, like those found in C_2. A direct calculation of the DI in these two cases provides the value 0.74 for diberyllium and 3.21 for dicarbon. This obviously indicates that the valence g,u functions interfere rather destructively. In fact, if the occupation threshold is relaxed, the situation changes. For instance, decreasing ε to 1.80 in Be_2 localizes all the electrons, although the valence localized functions extend considerably (10.3%) to the other center. This is shown in Fig. 1. Similarly, using $\varepsilon=1.62$ in dicarbon gives rise to distorted localized hybrids plus the common π Lewis pairs.

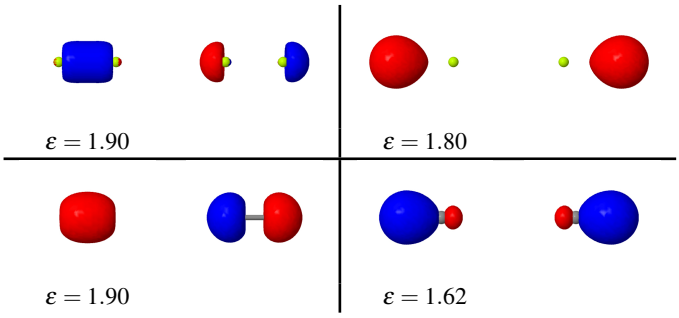

Fig. 1 $|\phi|=0.08$ a.u. isosurface of the 2σ-like valence functions of HF//cc-pVDZ descriptions of Be_2 (up) and C_2 (down). For each system, the left hand side functions are obtained if the occupation threshold $\varepsilon\approx1.90$ is used, and the right hand ones when ε is decreased down to $\varepsilon\approx1.80$ and $\varepsilon\approx1.62$ in Be_2 and C_2, respectively. The π functions in dicarbon are not affected in the process.

Notice that, interestingly, tuning the ε value may provide a set of different, non-conflicting bonding descriptions for a given system. In fact, the $\varepsilon=1.62$ image of C_2 is basically equivalent to that provided by the NBO technique in terms of a pair of σ $(v\bar{v})$ bonds and quadruple bonding.[25] This confirms the ability of the present position space electron counting method to recover ideas anchored in Fock space.

As a rule of thumb, playing with occupation thresholds is not needed in standard situations, and default ε values usually provide acceptable Lewis structures. It should be noticed that default thresholds are smaller than in NBO for very clear reasons. Real space occupations admit a simple interpretation in single-determinant cases. They measure exactly how many out of the nominal two electrons per function are contained in the n atomic basins. Since the (nc,ne) functions leak out of the strict union of basins that we are considering, the occupation thresholds need to be weaker than in NBO. When several Lewis structures may compete (these tend to be the interesting cases) some trial and error may be needed, as we have exemplified above. In general, the larger the number of electrons the final solution accounts for, the larger its physical soundness.

Let us also consider LiF (computed also at the HF//cc-pVDZ level) as an extreme case of ionic bonding. In this case, the one-center step of the rs-AdNCP algorithm exhausts the full set of electrons. $1s$-like cores are found in the Li and F centers together with four extra F-centered functions which we depict in Fig. 2. The eigenvalues of the $2s,2p_x,2p_y$ and $2p_z$ orbitals are $2.000, 1.986, 1.986$, and 1.958, respectively. Only the latter is slightly delocalized (2.1%) over the Li atom. This picture clearly corresponds to the standard ionic structure and becomes reinforced by noticing that the QTAIM net charge of F is -0.941 a.u. and that an electron distribution function analysis[51,53] (EDF) provides a probability of finding 10 electrons on F and 2 on Li equal to $p(10,2)=0.921$.

Inclusion of electron correlation provides further insight. We stress that our procedure is clearly different to that in NBO or AdNDP, where the first order density is always used, even in correlated situations. Here, correlated descriptions are obtained from the exchange-correlation density (Eq. 1), thus including true cor-

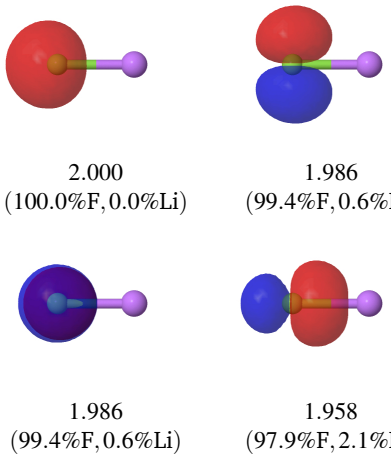

Fig. 2 $|\phi| = 0.08$ a.u. isosurface of the non-core one-center functions found in LiF at the HF//cc-pVDZ level. Notice, from left to right, the quasi-atomic nature of the F-centered $2s, 2p_x, 2p_y$ functions together with the clear polarization of the $2p_z$ one.

relation effects. In a full configuration interaction (FCI) calculation in Be_2 with the same basis set, for instance, the same two pictures shown above remain. If a large threshold is chosen, the cores are mostly unaffected, and the σ_g and σ_u valence functions retained, but now with non-integer occupation numbers, which decrease from 2.0 to 1.962 and 1.906 electrons, respectively. This is due to residual exchange-correlation density not accounted for by the standard Lewis structure. If a low threshold is selected, again a localized set appears, with valence localized orbitals showing occupations equal to 1.574 (1.709 in the HF case). The decrease in the total number of electrons accounted for with respect to the single-determinant HF case is a measure of the strength of electron correlation effects. The situation in dicarbon is rather similar. As we showed within a NAdOs description,[38] the $2\sigma_g, 2\sigma_u$ pair is to be understood at the root of recent debates on its purported quadruple bond.[54–56] Correlation considerably decreases the contribution to the DI of the ungerade function, this being translated in the present language to a smaller occupation number, 1.628 at the FCI level, while that of the $2\sigma_g$ orbital remains considerably populated, 1.968 electrons. As electron correlation becomes more and more intense, it is clear that some occupation numbers decrease, so that electron counting (or equivalently the value of simple Lewis structures) decreases. Thus, occupation thresholds need to be relaxed slightly when dealing with explicitly correlated wavefunctions.

Other interesting systems are transition metal dimers, where large scale multiple bonding has been invoked. To ascertain the role of electron correlation, we have performed high level heat bath configuration interaction (HCI)[57] calculations on Cr_2 with the cc-pwcVTZ basis set. The calculated DI is 2.757, far from the naïve bond order of six. This is well known, and as a system becomes more and more multireference in character, the DI decreases due to negative interference effects, i.e. to localization of pairs due to Coulomb correlation or to the increasing role of antibonding orbitals if a traditional view is held. However, the effect at the rs-AdNCP level is minor. Six (2c,2e) contributions are immediately found in pairs of σ, π, and δ symmetry, with occupations that add to 10.96 e. They are depicted in Fig. 3. Notice that the distance from 10.96 to 12 electrons is large, and can be understood as a measure of the multireference nature of this system. It is also interesting that each symmetry has a characteristic occupation window that decreases in the order $\sigma > \pi > \delta$, as expected. If we recall that the DI is directly related to the covalent energy component of a given interaction,[58] we come to the conclusion that a completely paired Lewis structure may be found with a sextuple bond which is compatible with a low covalent energy contribution coming from correlation induced electron localization.

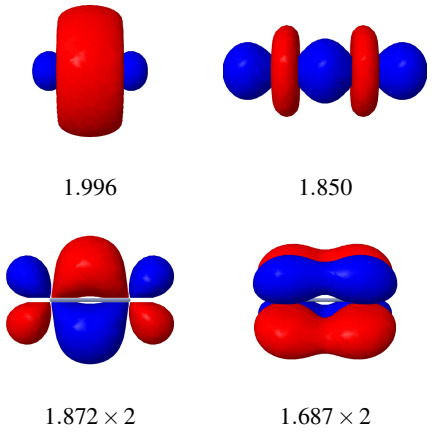

Fig. 3 $|\phi| = 0.06$ a.u. isosurface of the (2c,2e) contributions found in Cr_2. Details of the calculations are given in the text. In the upper panel the two σ functions are depicted, while in the lower a representative π (left) and δ (right) orbital are found.

Although we focus in this work on closed-shell examples, the rs-AdNCP algorithm can also be applied to open-shell systems. The Ne_2^+ and F_2^- are, for instance, paradigms of the (2c,3e) bond. We have performed B3LYP//TZV(d) calculations on both and examined the spin-resolved α and β channels, as explained above. Let us comment on Ne_2^+. As expected, the majority spin channel, in which the L atomic shells are filled, localizes completely after the rs-AdNCP procedure, giving rise to a set of quasi-atomic 2s and 2p functions in each atom with occupations larger than 1.99 for the $2p_{x,y}$ components and a bit smaller, but still large 1.97 value for the $2p_z$ one. The minority spin channel, on the contrary, displays the same localized 2s and $2p_{x,y}$ functions but a completely delocalized σp_z function with occupation exactly equal to 2.0. In this view, the (2c,3e) bond comes from a (2c,1e) contribution of the delocalized spin channel. If spinless cumulants are used, which is a perfectly legitimate, albeit less informative option in our opinion, symmetry broken solutions are found, and either Ne-Ne^+ or Ne^+-Ne Lewis structures appear. This is the standard resonance explaining these (3c,2e) bonds in Valence Bond approaches. Completely analogous results are found in the F_2^- anion.

Simple polyatomics

We examine now a few cases with well defined dominating Lewis structures taken from second period organic molecules. Fig. 4 shows the Lewis structure of ethylene at the HF//cc-pVDZ and quasi-FCI//cc-pVDZ levels, the latter obtained from a density matrix renormalization group (DMRG) calculation carried out using the PySCF suite[49]. DMRG[59] wavefunctions together with their density matrices, approaching the FCI level to better than 1 kcal/mol, were computed with the Block code[60–64], with all electrons and orbitals included.

Only two C one-center cores are found, the rest of the electrons being recovered at the two-center level. As seen, the degree of localization of the C-C and C-H σ bonds is similar, but the C-C π bond leaks slightly into the H atoms (1.6% its population lies within each of the four equivalent hydrogens). As in NBO descriptions, the polarity of two-center functions can be directly read. In our case, in terms of the percentage overlap of the orbitals in each atomic region.

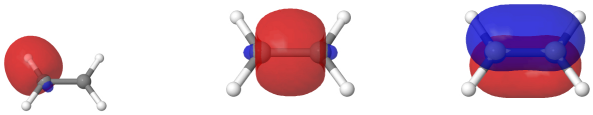

	HF	
1.967	1.966	1.870
(50.8%C,47.5%H)	(49.2%,49.2%)	(46.7%,46.7%)
	FCI	
1.931	1.932	1.781
(53.6%C,45.1%H)	(49.4%,49.4%)	(47.5%,47.5%)

Fig. 4 $|\phi| = 0.08$ a.u. isosurface of the non-core valence two-center functions found in ethylene at the HF//cc-pVDZ and quasi-FCI//cc-pVDZ levels. The shapes of the functions are only slightly altered in the two descriptions, so only the HF orbitals are shown. Only one C-H σ bond is reported. Two-center populations n^{ab} are also depicted, together with the percentage degree of localization of the functions in the two centers.

Notice that inclusion of correlation does not change the Lewis picture, although the existence of partially occupied orbitals in the multi-determinant case induces a slight decrease in the occupation numbers of the (2c,2e) functions. At this quasi FCI level, correlation induces a slight localization of both the σ and π C-C functions, as well as a contraction of the C-H orbitals toward the C end.

A similar analysis provides the $\sigma + 2\pi$ canonical description in acetylene. If we perform this time the analysis only at the FCI//cc-pVDZ correlated level, two C-H bonds with populations equal to 1.961 electrons (61.6%C,31.3%H), and a σ and two π C-C functions with occupations equal to 1.967 and 2×1.870 electrons, respectively, are found, but the latter delocalize slightly (0.9%) over each H atom. In this case, where a clear Lewis structure dominates again, correlation does not change the single-determinant image at all. It is also clear that the C-H function is considerably more C centered in acetylene than in ethylene, in agreement with electronegativity arguments or with the NBO hybrid structure.

To exemplify the role of lone pairs, our next example is methanol, where we have performed the rs-AdNCP analysis at the CCSD(T)//cc-pVDZ level. Besides the 1s cores, two extra one-center functions are found centered on the oxygen atom. As it occurs in NBO or AdNDP analyses, the density matrix which is diagonalized (in our case ρ^a for each atom) has the point group symmetry of the atom in which it is obtained. Similarly, the two-center functions possess the symmetry of the bond, and so on. This means that lone pairs will belong to the irreducible representations of the atomic point group. For oxygen, the σ plane forces a pair of symmetric and antisymmetric lone pairs. These are shown in Fig. 5. In order to obtain a tetrahedral arrangement of the pairs, like that found when examining $\nabla^2\rho$, for instance, one can perform an isopycnic localization.[65] We will not pursue this goal here. The considerably polar nature of the O-H and C-O bonds is also clear from the analysis.

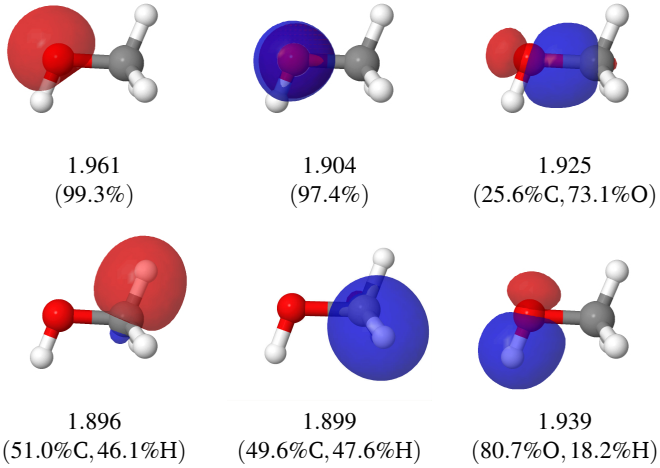

1.961	1.904	1.925
(99.3%)	(97.4%)	(25.6%C,73.1%O)
1.896	1.899	1.939
(51.0%C,46.1%H)	(49.6%C,47.6%H)	(80.7%O,18.2%H)

Fig. 5 $|\phi| = 0.08$ a.u. isosurface of the non-core valence 1c and 2c functions found in methanol at the CCSD(T)//cc-pVDZ level. Two-center occupations and percentage of population localized are also shown as in Fig. 4.

The last example on simple Lewis structures is provided by formic acid. Only the oxygens' lone pairs and the π system of the -COOH group computed at the HF//cc-pVDZ level are shown in Fig. 6. As expected, and as it can be corroborated by the ELF or the Laplacian of the density, the two lone pairs of the carbonylic oxygen lie in the molecular plane. An isopycnic localization would mix them, if desired. What is interesting here is to point out the nature of the p- or π-like lone pair of the hydroxylic oxygen. If $\varepsilon = 1.84$, as depicted, then this is found at the 1c step as a lone pair centered on oxygen, with occupation equal to 1.886. Using $\varepsilon > 1.886$ will lead to consider this pair as a two center function, paving the way to a three-center delocalization with the other carbonylic π orbital. This will be clearly shown when we examine the formate anion in the next subsection*. Repeating the rs-AdNCP analysis of formic accid, this time at the CCSD(T)//cc-pVDZ level and using $\varepsilon = 1.80$, the lone pair of the hydroxylic oxygen is found at the 1c step with an occupation equal to 1.804, to be compared with the value found at the HF level (1.886). It is worth noting that when $\varepsilon = 1.84$ is used in the correlated calculation, the σ bond between the hydroxylic oxygen and the acidic

hydrogen has an occupation (1.865) smaller than that found for a three-centered π MO between both oxygen atoms (1.909).

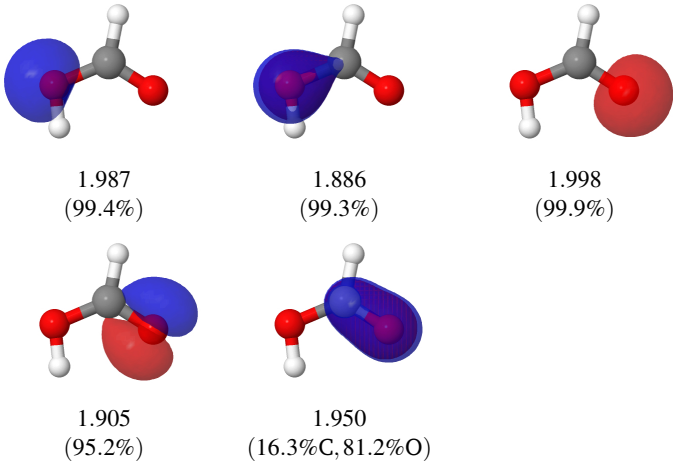

Fig. 6 $|\phi| = 0.08$ a.u. isosurface of the non-core valence 1c and 2c functions found in the -COOH group of formic acid at the HF//cc-pVDZ level. The C-O and O-H σ functions have been omitted. Two-center occupations are also shown. The ε value has been set to 1.84. At this level, only the last function is obtained in the two-center step.

We end this subsection by showing how the rs-AdNCP algorithm may be used in slightly larger cases. Anion-π interactions have been much discussed in recent years,[66] and doubts exist about the ionic or multi-center nature of their binding. We have computed the complex of the Cl^- anion with hexafluorobenzene in its on-top conformation at the M06-2x//def2-qzVPD level. This is enough for our purposes here. Standard ε thresholds provide a very clear image with four valence (1c,2e) functions for the chloride anion which are clearly compatible with an anionic Lewis picture, this not impeding a certain degree of covalency. Actually, the chloride $3p_z$ function is clearly polarized, as shown in Fig. 7. The QTAIM net charge of Cl^- is -0.946 e, and the total DI between the chloride and the hexafluorobenzene is 0.269, typical of an ionic interaction. The associated IQA covalent contribution is -12 kcal/mol.

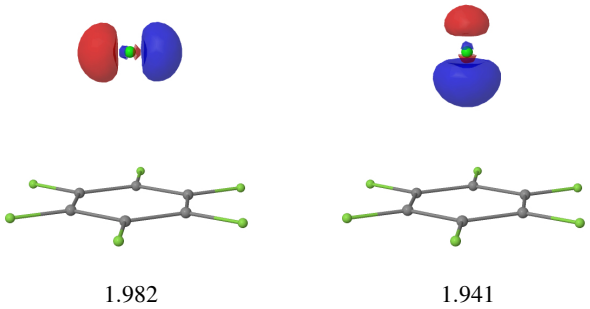

Fig. 7 $|\phi| = 0.1$ a.u. isosurface of the chloride valence functions found for the $ClC_6F_6^-$ complex. Details of the calculations are given in the text. We show the $3p_x$ (left, equivalent to $3p_y$) and $3p_z$ (right) functions.

Multicenter bonding cases

We start our presentation of the performance of the method in multi-center bonding cases by examining diborane, B_2H_6, at the HF//cc-pVDZ level. Setting $\varepsilon = 1.80$ we obtain the standard description in terms of four (2c,2e) σ B-H_t functions and two (3c,2e) B-H_b-B links (t stands for terminal, and b for bridge). However, the QTAIM description of B_2H_6 gives rise to considerably charged atoms. At the HF level, the QTAIM net charges of B, H_t and H_b atoms are $1.990, -0.664$, and -0.659 a.u., respectively. In this sense, as expected from electronegativity differences, hydrogens are on their way to becoming hydrides, being thus large, polarized entitities. The fluctuation of electron populations, as measured by the delocalization indices (DIs) is also informative. The B-B, B-H_t, B-H_b, vicinal H_t-H_t and H_b-H_b DIs are, respectively, $0.068, 0.520, 0.300, 0.125, 0.107$. Notice that the B-$H_b$ direct delocalization channel is only three-times stronger than the H_b-H_b one. Along with the orthodox Lewis structure of diborane, secondary interactions are non-negligible in this type of systems. This has already been put forward.[67] In the present context, this means that it is very easy to recover different Lewis structures on varying ε. For instance, Fig. 8 shows that the multi-center

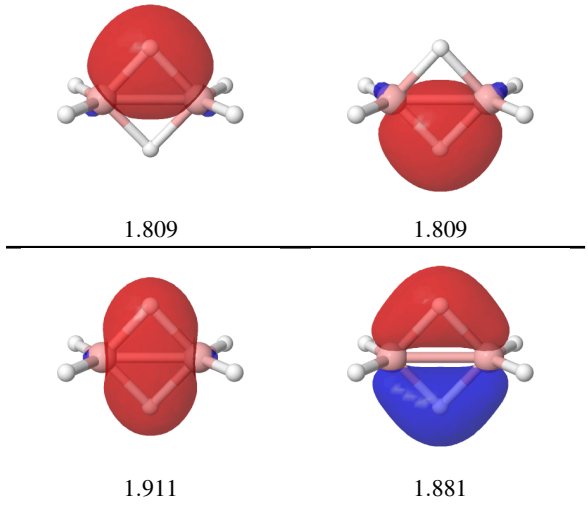

Fig. 8 $|\phi| = 0.08$ a.u. isosurface of the orbitals that include the H_b atoms in diborane, together with their occupation numbers. At $\varepsilon = 1.80$ (top) two (3c,2e) bonds are found, while at $\varepsilon = 1.86$ (bottom) two (4c,2e) bonds describe the whole bridge.

character of the bonds in the bridge may change easily from two 3-center bonds, with no direct H_b-H_b interaction, to two 4-center bonds. The occupation numbers of the functions, as found in the figure, add up to only a slightly larger value in the four-center description (3.79 versus 3.62 electrons). This is due to considerable charge leak over the rest of the molecule. The (3c,2e) orbitals are localized 72.0% and 9.3% over the H_b and B atoms, 3.5% over the opposing H_b (this being related to the large H_b-H_b DI), and 6.4% globally over the terminal hydrogens. In the four-center description, the delocalization of the three-center bonds over the opposing bridging atom is absorbed by building in-phase and out-of-phase combinations, which are essentially equivalent

to a pair of the HF canonical orbitals. These (4c,2e) functions are localized 36.8% and 11% over the H_b and B atoms in the gerade combination, respectively, and 38.8%, 7.2% in the ungerade one, in the same order.

Actually, the modelling here is too restrictive, since we are dealing with a set of four electrons delocalized in four centers, a situation which should be described as a (4c,4e) link. We have no good pictorial representation of anything beyond an electron pair, a fact that forces considering this $(n > 2)$e bonds in terms of independent pairs, although a classification migth be possible in terms of EDFs. Similar comments apply to benzene, which will be discussed below.

When several competing Lewis structures are at stake, the general rule to choose one over the others should be the total electron count, the larger the better. Notice, however, that a trade between chemical soundness and electron count is at some point needed. In single determinant closed-shell cases, for instance, it is clear that the original canonical orbitals (and any of their infinite unitary transformations) lead to an exact electron count from the start, without any transformation. This is also true of NBO and AdNDP. In single determinant (or pseudo-determinant) cases it is also possible to construct a Slater determinant from the different Lewis structures at stake and compare their energies, much like it is done in the NBO framework. We have not undertaken such an enterprise in this introductory paper.

If the ε thresholds are tightened even more, then the (2c,2e) B-H_t bonds, which are localized 77.8%, 16.1% over the B,H_t pairs and 2.0%, 1.9%, 1.9% over the companion H_t atom and the bridging hydrogens, become also multi-centered. This discussion highlights the power and the limits of NBO-like reasoning and of the (nc,2e) bond concept.

Applying the algorithm to HF//cc-pVDZ benzene leads to a set of carbon cores and (2c,2e) σ bonds for all the C-C and C-H pairs. This leaves about six electrons that can be localized in a rather large variety of ways, as it occurs in other procedures (i.e. with the Pipek-Mezey[6] algorithm). We can get three (2c,2e) Kekulé-like pairs in their two possible motifs, in agreement with the textbook resonance, or several arrangements of three-center bonds, for instance. Again, we have a well-defined (6c,6e) situation that is forced to fit in terms of three independent pairs, leading to a plurality of equivalent descriptions.

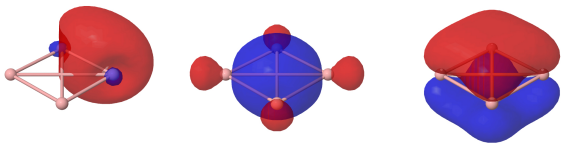

Fig. 9 $|\phi| = 0.08$ a.u. isosurface of one of the four equivalent peripheral (2c,2e) bonds in the B_4 cluster together with the two (4c,2e) aromatic channels. Occupancies are also detailed.

More interesting cases, for which the AdNDP or rs-AdNCP recipes show a clear superiority over the normal NBO scheme are exemplified by small metallic clusters. We will consider the B_4 and B_5^- aggregates in their ground state optimized geometries at the HF//aug-cc-pVDZ and B3LYP//6-311G* levels, respectively. In the former, with a D_{2h} ^1A_g state, Fig. 9 shows that the valence electrons may be well described by a set of four (2c,2e) peripheral bonds and two completely delocalized (4c,2e) aromatic channels of σ and π symmetry. This is virtually the same description as that reported from Fock-based AdNDP procedures.[27] Instead of the four fully delocalized electrons, a standard NBO analysis gives rise to eight lone pairs with occupation close to 0.5 electrons, which have no direct chemical interpretation. We think that the (4c,2e) description of both AdNDP and rs-AdNCP will be also found with NBO if larger order multi-center bonding is allowed.

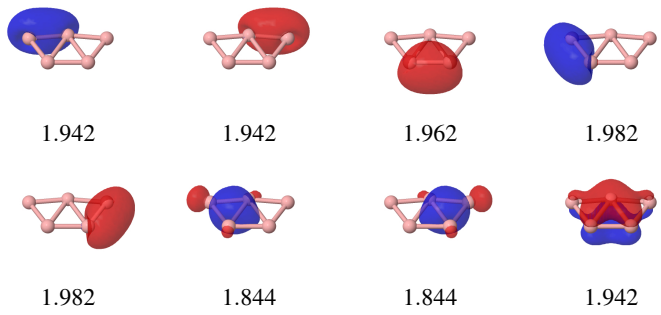

Fig. 10 $|\phi| = 0.08$ a.u. isosurface of the two- to five-centered functions in B_5^-. Occupancies are also detailed.

A similar case is that of the B_5^- anion,[27] another of the prototypes in which NBO provides a set of low occupancy functions difficult to rationalize from the chemical point of view. The C_{2v} $^1A_1$ ground state provides canonical orbitals which are interpreted in terms of conflicting aromaticity with an antiaromatic σ skeleton coming from two occupied orbitals plus an aromatic π delocalized fragment. A set of reasonable ε thresholds, 1.96, 1.92, 1.84, 1.84, 1.84 for the $n = 1 \ldots 5$ steps of the procedure provides the same image found with AdNDPs. Five (2c,2e) peripheral orbitals differing in their localization degrees are found. In agreement with the AdNDP paritioning, the highest occupancies are those of σ functions linking the left and right boron pairs, which are slightly polarized (54.5%, 44.7%) toward the lower atom. With occupancies slightly smaller than these ones, we find a (2c,2e) bond that links the two B atoms found in opposition to the appex of the pentagon. Actually, the two bonds connecting the apical atom to the borons at the corners have a clear lone pair contribution, being polarized against the appical atom (55.0%, 42.2%), and becoming isolated as lone pairs if more stringent thresholds are used. Upon this, two (3c,2e) contributions appear which have lower occupancies (as in AdNDP). They may be interpreted as antiaromatic σ islands, and leave about two electrons for a totally symmetric (5c,2e) delocalized canonical orbital.

At this point we want to caution against taking Lewis interpretations too far. For instance, an ELF analysis of the same B_5^- Kohn-Sham pseudodeterminant is found to locate two clear lone pairs, with attractor $\eta \approx 0.982$, as visualized in Fig. 11. At lower η values, the peripheral bonds appear, in rather exo positions with

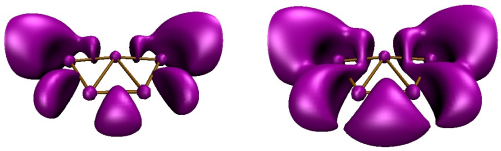

Fig. 11 ELF isosurfaces at $\eta = 0.88$ (left) and $\eta = 0.80$ (right), showing the fusing of the lone pairs with the apical to corner B-B bond domains and the formation of the three-center islands.

respect to the wire framework. This is also found from examining the bond critical points of the density and from the outwards features of the above (2c,2e) functions. Notice that the lone pairs fuse with the apical to corner B-B bonding ELF domains. If η is decreased at about a value close to 0.80 the two three-center islands are retreived.

We have found that the present method can recover basically all the insights into the multi-center bonding of small boron clusters described by the AdNDP methodology. They will not be analyzed any further.

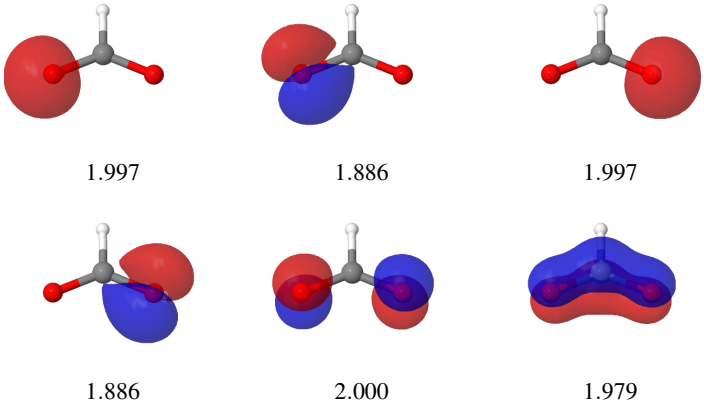

Fig. 12 $|\phi| = 0.08$ a.u. isosurface of the valence two- and three-center functions in the formate anion. The C-H and C-O σ bonds have been omitted. Occupancies are also detailed.

We end this subsection by showing B3LYP//6-311G(d,p) results in the formate anion. This is an interesting example, since two very similar descriptions are available. If thresholds are set to $\varepsilon = 1.84$, a two-center localized image is found, with standard σ lone pairs on the oxygens and two equivalent (2c,2e) C-O π bonds. We can surely obtain a three-center picture of the -COO^- π system. However, this has to be done with care, since the above-mentioned lone pairs are relatively delocalized over the C atoms (3.3%). If (3c,2e) orbitals are forced, their occupancies turn out to be equal to 1.98 electrons, a figure to be compared to the 1.96 occupation of their (2c,2e) counterparts. Actually the total electron population accounted for by both descriptions differs only in 0.1 electrons in favor of the multi-center bonding.

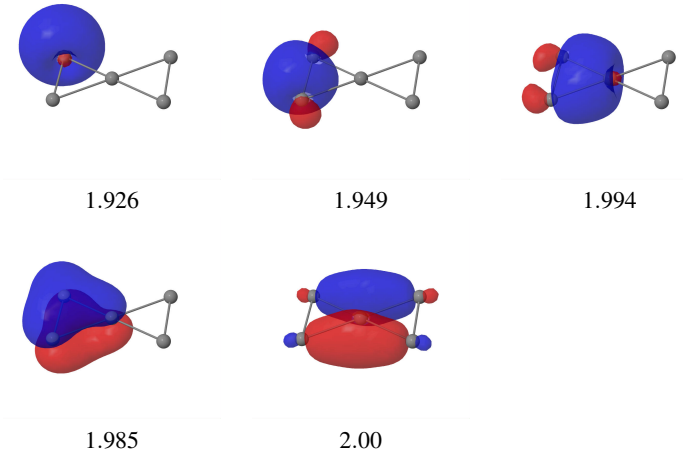

Fig. 13 $|\phi| = 0.08$ a.u. isosurface of the lone pair, (2c,2e), (3c,2e), (5c,2e) valence functions in the planar C_5^{2-} anion. Occupancies are also detailed. Only one of the lone pairs, σ (2c,2e), π (2c,2e), and π (2c,2e) functions, as well as the (5c,2e) function, are shown.

Exotic systems

In this last subsection, we summarize the results found for the C_5^{2-},[68] C_5H_4,[68] and CAl_3P[69] systems, all of them displaying a planar tetracoordinated carbon atom, as well as the pentagonal-pyramidal hexamethylbenzene dication, $C_6(CH_3)_6^{2+}$, characterized by a hexacoordinated carbon.[70] The geometry optimization and rs-AdNCP analyses of the first three were carried out using the Density Functional Theory (DFT) with the Chai and Head-Gordon range-separated functional wB97X-D, which includes atom-atom dispersion corrections,[71] and the def2-tzvpd basis set. In the case of the $C_6(CH_3)_6^{2+}$ dication (Table 1), the rs-AdNCP analysis was performed at the wB97X-D//def2-tzvpd level with the geometry optimized using the wB97X-D//def2-svpd basis set. Fig. 13 shows the valence functions of C_5^{2-}. Despite the exotic coordination of the central C, the Lewis structure of this system is simple and clear. Together with the four equivalent lone pairs in the outer C's, we find a (2c,2e) C-C σ bond in the left and right C_2 pairs with occupancy 1.949, two (3c,2e) bonds, one σ and one π, in the left and right C_3 trios with occupancies 1.994 and 1.985, and a (5c,2e) π bond. Each (3c,2e) σ function is localized 53% and 23% in the central in each of the outer carbon atoms, respectively, while the π one is more localized in the outer C's (37%) than in the central carbon (25%). It is worth noting that no σ (2c,2e) functions between the central carbon atom and the outer ones are detected, regardless the threshold value chosen for ε.

The C_5H_4 molecule adds two electrons over the C_5^{2-} cation, so that we have twelve valence functions (see Fig. 14). The lone pairs of the outer C's in C_5^{2-} transform to standard (2c,2e) σ C-H bonds with occupancy 1.982, while the (2c,2e) C-C σ functions are retained in C_5H_4 with a slightly larger occupancy (1.974). The rest of the Lewis pairs differ in some aspects from those found in C_5^{2-}. For instance, besides the (2c,2e) σ bond in the left and right C_2 pairs, each of these pairs displays also a (2c,2e) π function with occupancy 1.903. It also seems that each (3c,2c) π func-

tion in C_5^{2-} has transformed into a (2c,2c) π function in C_5H_4 by decreasing the degree of localization from 25% to 2.3% in the central carbon atom. The (3c,2e) σ bonds in the left and right carbon trios of C_5^{2-} are also obtained here, although with a considerable decreased occupancy (1.981). Actually, each (3c,2e) σ bond, if plotted with an isosurface value of $|\phi| = 0.09$ a.u., instead of the 0.08 value used in Fig. 14, looks like a superposition of two (2c,2e) σ bonds between the central carbon and each of the two left (or right) C atoms. The (5c,2e) function found in C_5^{2-} dissapears in C_5H_4. Instead, we have two equivalent (3c,2e) σ bonds between the central C atom and the upper and lower carbon pairs. These two (3c,2e) bonds, as well as the other two (3c,2e) σ functions commented above, are significantly more localized in the central C atom than in the outer ones.

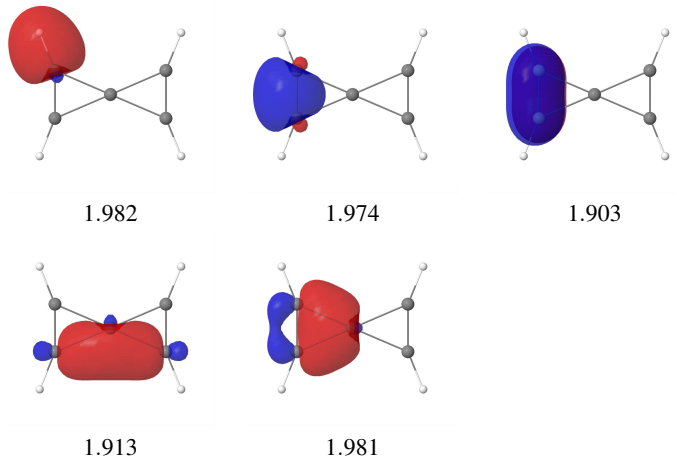

Fig. 14 $|\phi| = 0.08$ a.u. isosurface of the (2c,2e) and (3c,2e) functions in planar C_5H_4. Occupancies are also detailed. Only one of the four equivalent σ C-H bonds, the σ and π functions in the left C-C pair, and the three-center functions in the lower and left trios of carbon atoms, are shown.

CAl_3P is our next system. The underlying QTAIM calculation displays a slightly positively charged P atom ($Q = +0.37$ au), together with highly charged Al units ($Q = +0.77$). This leads a heavily negative C atom behind. Simple bond paths are found between the central atom and the outer ligands, with no path among the latter. The density at the C-P critical point, 0.18 au, points toward a well established carbon-phosphorous link, while that between the C and each of the Al atoms (0.06) is consistent with their closed-shell character. Taking out the cores we are left with nine valence functions. We have found that quite a number of similar rs-AdNCP descriptions, different marginally in the sum of eigenvalues, can be found. We show in Fig. 15 one of these rs-AdNCP distributions. A clear phosphorous lone pair appears together with three quasi-lone pairs at each Al atom that delocalize over the carbon. A very clear C-P double bond with σ and π components can also be distinguished. The C atom can be read in terms of a close to sp^2+p configuration, using one of the hybrids to form the C-P σ link, that leaves two hybrids to form close to (3c,2e) links with each of the lateral Al_2 units (they are asymmetric and more localized on one of the Al atoms than on the other). A final C-Al (2c,2e) σ bond completes the picture, justifying the shorter vertical C-Al distance and its associated larger critical point density. Overall, the P atom bears a formally +1 charge in the Lewis structure, compensated at the C end. If the aluminums are also assigned a formal +1 charge, the C octet is filled up.

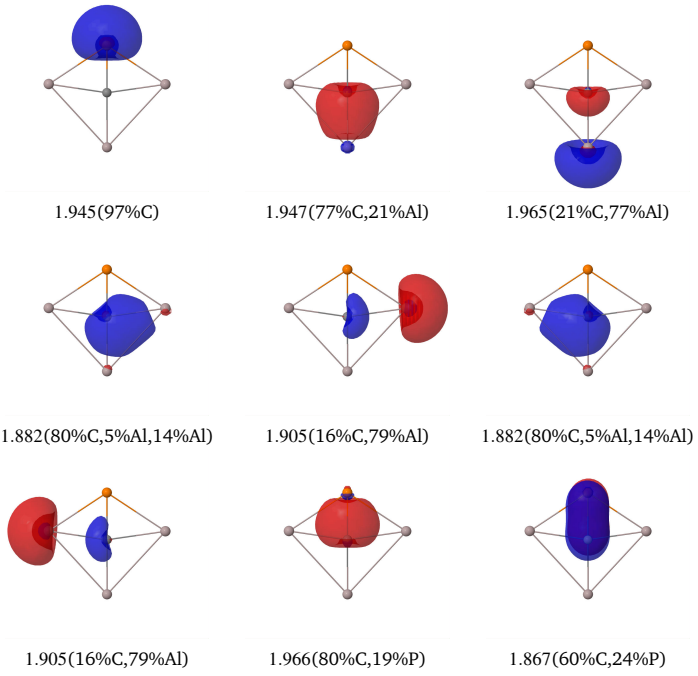

Fig. 15 $|\phi| = 0.08$ a.u. isosurface of lone pair, (2c,2e) and (3c,2e) valence functions in planar CAl_3P. Occupancies and degrees of localization of all the functions in the different atoms are also detailed.

We have searched for (2c,2e) and (nc,2e) ($n \geq 3$) bonds in the cation $C_6(CH_3)_6^{2+}$ (Fig. 16), using the thresholds $\varepsilon = 1.90$ and $\varepsilon = 1.80$, respectively. No (2c,2e) bonds are detected between the equatorial carbon atoms (C_{eq}) in the pyramid and the apical one (C_{ap}), and the simplest Lewis structure is built from standard (2c,2e) C-C_{methyl} and C-H bonds and three (3c,2e) bonds that link the apical C in the pyramid with two equatorial carbons, with details that can be found in Table 1. Since this number of bonds is incommesurate with the symmetry of the pyramid, we face a situation similar to that of benzene, and now there are $\binom{5}{3} = 20$ almost equivalent distributions of the trio of bonds over the pyramid. As in benzene, this shows that we should consider a (6c,6e) bond, in perfect agreement with the consideration of this cation as a case of three-dimensional atomaticity.[72]

Each of the (3c,2e) functions, as the three in Table 1, is localized around 41% in C_{ap} and 25% in each of two C_{eq}'s, with a rather small overlap in the other three equatorial carbons. We have also determined the DIs between C_{ap} and the five C_{eq}'s, as well as between C_{ap} and the carbon atom above it, finding values of about 0.58 in the first case and 1.01 in the second. This gives a total bond order of C_{ap} with its six neighbors equal to 3.9, confirming that, despite its hypercoordination, the apical carbon is not hypervalent[72].

function	occ	C_{ap}	$C_{eq,1}$	$C_{eq,2}$	$C_{eq,3}$	$C_{eq,4}$	$C_{eq,5}$
1	1.82	41.4	24.7	25.4	2.2	2.1	1.7
2	1.82	41.4	24.7	2.1	1.7	25.4	2.2
3	1.82	41.2	1.7	2.2	24.9	2.2	25.3

Table 1 Electron occupancies (column 2) and degrees of localization of one of the possible sets of three (3c,2e) functions found between the apical carbon atom, C_{ap}, and the five equatorial carbon atoms, $C_{ap,i}$ $(i = 1,5)$ in the $C_6(CH_3)_6^{2+}$ cation.

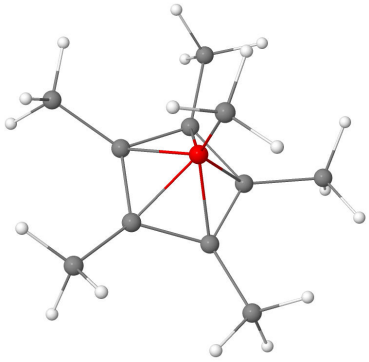

Fig. 16 The $C_6(CH_3)_6^{2+}$ cation with the hexacoordinated carbon atom in red.

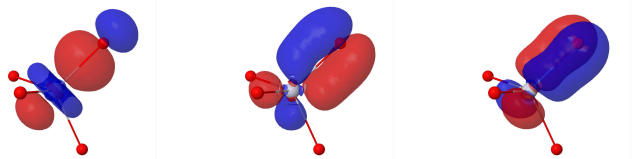

Fig. 17 $|\phi| = 0.08$ a.u. isosurface of the (2c,2e) Pt-O functions in PtO_4^{2+} complex. Only one Pt-O pair is shown. Occupancies and degrees of localization of the three functions in the Pt,O pair of atoms are also detailed.

The tetrahedral PtO_4^{2+} complex

This tetrahedral cation has aroused interest lately due to the alleged X oxidation state of platinum.[73] We have carried out Heat-Bath Configuration Interaction (HCI) calculations[57] on this system with a 10^{-3} E_h threshold and using the Automated Construction of Molecular Active Spaces (AVAS) method (with 24 electrons in 17 valence orbitals),[74] as implemented in the PySCF suite.[49] The resulting wavefunction provides $Q_{Pt} = 2.84$, $Q_O = -0.21$, and was analyzed with the rs-AdNCP procedure using the threshold $\varepsilon = 1.90$. Out of the 54 two-electron functions, 42 of them are practically monocentric (34 localized in the Pt atom and 2 in each oxygen atom with an almost pure 1s and 2s character). The remaining twelve functions are of the (2c,2e) type, distributed into four equivalent sets of one σ and two degenerate π Pt-O bonds, see Fig. 17. These are basically obtained from Pt d functions and oxygen 2p orbitals. The degrees of localization of each (2c,2e) function in the Pt atom (43%σ,40%π) are slightly smaller than in the O atom (56%σ,58%π), a result compatible with the small charges of the oxygens. Overall, the sum of the rs-AdNCP eigenvalues leaves less than one electron remaining to account for dynamical correlation and multi-center bonding effects. An electron distribution function analysis[51,53] shows that the most probable electron distributions is $Pt^{+2}O_4^0$, with Pt,O delocalization index of about $1.29-1.30$. There is a negligible value ($< 10^{-5}$) for the probability of the four oxygen atoms displaying simultaneously a net charge of -2, and a probability smaller than 2.2% that a single O atom has a negative net charge of -1. These facts seem to indicate that the formal oxidation number of Pt is far from being reflected by the electronic structure of the system.

Conclusions

Position space narratives in the theory of chemical bonding possess the intrinsic advantage of being based on orbital invariant descriptors, thus being immune to the interpretation biases that are inherent to any computational framework used to build a molecule's wavefunction. However, lacking orbitals, they have not been immediately adopted by the Chemistry community. In recent years, several proposals that construct effective one electron functions from real space indicators, like the domain natural orbitals of Ponec and coworkers,[42,43] or the generalization provided by our natural adaptive orbitals[38] have appeared that ease the transition from an orbital picture to a real space one. However, none of these provide a simple electron counting mechanism or gives rise to simple Lewis images. We have shown in this paper how the adaptive natural density partitioning proposed by Zurek and Boldyrev,[27] a generalization of the well known natural bond orbital approach of Weinhold and collaborators,[22–25] can be reframed into real space through the use of domain-averaged cumulants. The simplest hierarchy coming from our real space adaptive natural cumulant partitioning (rs-AdNCP) uses the second order cumulant, or exchange-correlation density. This is domain-averaged and diagonalized in each atomic center, described from QTAIM basins, in a first step, and depleted from large occupancy functions in a second one. The procedure is iterated for two centers, three, etc, until all electrons to a given threshold have been exhausted. Both single and multi-determinant wavefunctions can be used.

As shown through several examples, from simple molecules described correctly with (2c,2e) Lewis structures to others in which accounting for multi-center bonding is essential, the present rs-AdNCP framework reproduces essentially the AdNDP results in archetypal systems, showing that NBO-like arguments, Lewis structure searches and electron counting techniques can be

equally obtained from orbital invariant real space analyses. Moreover, our procedure generates a complete hierarchy that may account for true many-particle correlations if further order cumulant densities are used. These are however computationally intensive objects which are not easily accessible. We leave this enterprise for future work.

Acknowledgements

We thank the spanish MINECO/FEDER, grant CTQ2015-65790-P, and the FICyT, grant GRUPIN14-049. The authors are also very grateful to José Luis Casals–Sainz for his valuable help in generating the wavefunctions of some of the systems that have been used in this work.

References

1 G. N. Lewis, *J. Am. Chem. Soc.*, 1916, **38**, 762–786.
2 M. Kaupp, *Chem. Bond Chem. Bond. Across Period. Table*, 2014, pp. 1–24.
3 B. M. Gimarc, *Molecular structure and bonding. The qualitative molecular orbital approach*, Academic Press, New York, 1979.
4 J. M. Foster and S. F. Boys, *Rev. Mod. Phys.*, 1960, **32**, 300–302.
5 C. Edmiston and K. Ruedenberg, *Rev. Mod. Phys.*, 1963, **35**, 457–465.
6 J. Pipek and P. G. Mezey, *J. Chem. Phys.*, 1989, **90**, 4916–4926.
7 F. Aquilante, T. B. Pedersen, S. de Merás and H. Koch, *J. Chem. Phys.*, 2006, **125**, 174101.
8 S. Lehtola and Jónsson, *J. Chem. Theory Comput.*, 2013, **12**, 5365–5372.
9 S. Lehtola and Jónsson, *J. Chem. Theory Comput.*, 2014, **10**, 642–649.
10 A. Heßelmann, *J. Chem. Theory Comput.*, 2016, **12**, 2720–2741.
11 I.-M. Høyvik and P. Jørgensen, *J. Chem. Theory Comput.*, 2012, **8**, 3137–3146.
12 I.-M. Høyvik, J. Branislav and P. Jørgensen, *J. Comput. Chem.*, 2013, **34**, 1456–1462.
13 I.-M. Høyvik and P. Jørgensen, *Chem. Rev.*, 2016, **116**, 3306–3327.
14 G. Knizia, *J. Chem. Theory Comput.*, 2013, **9**, 4834–4843.
15 S. S. Shaik and P. C. Hiberty, *A Chemist's Guide to Valence Bond Theory*, Wiley, 2007.
16 S. Shaik, D. Danovich, W. Wu and P. C. Hiberty, *Nat. Chem.*, 2009, **1**, 443–449.
17 S. Shaik, D. Danovich, W. Wu, P. Su, H. S. Rzepa and P. C. Hiberty, *Nat. Chem.*, 2012, **4**, 195–200.
18 S. Shaik, H. S. Rzepa and R. Hoffmann, *Angew. Chem. Int. Ed.*, 2013, **52**, 3020–3033.
19 D. Danovich, S. Shaik, H. S. Rzepa and R. Hoffmann, *Angew. Chem. Int. Ed.*, 2013, **52**, 5926–5928.
20 D. Danovich, P. C. Hiberty, W. Wu, H. S. Rzepa and S. Shaik, *Chem. Eur. J.*, 2014, **20**, 6220–6232.
21 W. H. Eberhardt, B. Crawford and W. N. Lipscomb, *J. Chem. Phys.*, 1954, **22**, 989–1001.
22 A. E. Reed, L. A. Curtiss and F. Weinhold, *Chem. Rev.*, 1988, **88**, 899–926.
23 A. R. Reed and F. Weinhold, *J. Chem. Phys.*, 1983, **78**, 4066–4073.
24 A. R. Reed, F. Weinhold, L. A. Curtiss and D. J. Pochatko, *J. Chem. Phys.*, 1986, **84**, 5687–5705.
25 F. Weinhold and C. Landis, *Valency and Bonding. A Natural Bond Orbital Donor-Acceptor Perspective*, Cambridge Univ. Press, 2005.
26 A. E. Reed and F. Weinhold, *J. Chem. Phys.*, 1985, **83**, 1736–1740.
27 D. Y. Zubarev and A. I. Boldyrev, *Phys. Chem. Chem. Phys.*, 2008, **10**, 5207–5217.
28 D. Y. Zubarev and A. I. Boldyrev, *J. Phys. Chem. A*, 2009, **113**, 866–868.
29 A. P. Sergeeva and A. I. Boldyrev, *Comments Inorg. Chem.*, 2010, **31**, 2–12.
30 W. Huang, A. P. Sergeeva, H.-J. Zhai, B. B. Averkiev, L. S. Wang and A. I. Boldyrev, *Nat. Chem.*, 2010, **2**, 202–206.
31 I. A. Popov and A. I. Boldyrev, *Eur. J. Org. Chem.*, 2012, **2012**, 3485–3491.
32 D. Y. Zubarev, A. P. Sergeeva and A. I. Boldyrev, *Chemical Reactivity Theory: A Density Functional View*, CRC Press. Taylor & Francis Group, New York, 2009, ch. 29, pp. 439–452.
33 E. Francisco, A. Martín Pendás, M. García-Revilla and R. Álvarez Boto, *Comput. Theor. Chem.*, 2013, **1003**, 71–78.
34 A. D. Becke and K. E. Edgecombe, *J. Chem. Phys.*, 1990, **92**, 5397–5403.
35 R. F. W. Bader, *Atoms in Molecules*, Oxford University Press, Oxford, 1990.
36 M. A. Blanco, A. Martín Pendás and E. Francisco, *J. Chem. Theory Comput.*, 2005, **1**, 1096–1109.
37 E. Francisco, A. Martín Pendás and M. A. Blanco, *J. Chem. Theory Comput.*, 2006, **2**, 90–102.
38 M. Menéndez, R. Ávarez Boto, E. Francisco and A. Martín Pendás, *J. Comput. Chem.*, 2015, **36**, 833–843.
39 E. Francisco, A. Martín Pendás, M. García-Revilla and R. Álvarez Boto, *Comput. Theor. Chem.*, 2013, **1003**, 71–78.
40 W. Kutzelnigg and D. Mukherjee, *J. Chem. Phys.*, 1999, **110**, 2800–2809.
41 P.-O. Löwdin, *Phys. Rev.*, 1955, **97**, 1474–1489.
42 R. Ponec, *J. Math. Chem.*, 1997, **21**, 323–333.
43 R. Ponec, *J. Math. Chem.*, 1998, **23**, 85–103.
44 E. Francisco, A. Martín Pendás and M. A. Blanco, *J. Chem. Phys.*, 2009, **131**, 124125.
45 E. Francisco, A. Martín Pendás and A. Costales, *Phys. Chem. Chem. Phys.*, 2014, **16**, 4586–4597.
46 R. Ponec and D. L. Cooper, *Faraday Discuss.*, 2007, **135**, 31–42.
47 D. Bonchev and D. H. Rouvray, *Chemical Graph Theory: Introduction and Fundamentals*, CRC Press, New York, 1991.
48 M. W. Schmidt, K. K. Baldridge, J. A. Boatz, S. T. Elbert, M. S.

Gordon, J. H. Jensen, S. Koseki, N. Matsunaga, K. A. Nguyen, S. J. Su, T. L. Windus, M. Dupuis and J. A. Montgomery, *J. Comput. Chem.*, 1993, **14**, 1347–1363.

49 Q. Sun, T. C. Berkelbach, N. S. Blunt, G. H. Booth, S. Guo, Z. Li, J. Liu, J. McClain, S. Sharma, S. Wouters and G. K.-L. Chan, *The Python-based Simulations of Chemistry Framework (PySCF)*, http://arxiv.org/abs/1701.08223, 2017.

50 A. Martín Pendás and E. Francisco, *Promolden: A QTAIM/IQA code (Available from the authors upon request by writing to ampendas@uniovi.es)*.

51 E. Francisco and A. Martín Pendás, *Comput. Phys. Commun.*, 2014, **185**, 2663 – 2682.

52 *WebBook, NIST Standard Reference Database Number 69*, National Institute of Standards and Technology, Gaithersburg MD, 20899, 2017.

53 E. Francisco, A. Martín Pendás and M. A. Blanco, *J. Chem. Phys.*, 2007, **126**, 094102.

54 S. Shaik, D. Danovich, B. Braida and P. C. Hiberty, *Chem. Eur. J.*, 2016, **22**, 4116–4128.

55 G. Frenking and M. Hermann, *Chem. Eur. J.*, 2016, **22**, 18975–18976.

56 D. W. Oliveira de Sousa and A. C. Nascimento, *J. Chem. Theory Comput.*, 2016, **12**, 2234–2241.

57 A. A. Holmes, H. J. Changlani and C. J. Umrigar, *J. Chem. Theory Comput.*, 2016, **12**, 1561–1571.

58 A. Martín Pendás and E. Francisco, *Phys. Chem. Chem. Phys.*, 2018, **20**, 16231–16237.

59 G. K.-L. Chan and D. Zgid, *Annu. Rep. Comput. Chem.*, 2009, **5**, 149–162.

60 G. K.-L. Chan and M. Head-Gordon, *J. Chem. Phys.*, 2002, **116**, 4462–4476.

61 G. K.-L. Chan, *J. Chem. Phys.*, 2004, **120**, 3172–3178.

62 D. Ghosh, J. Hachmann, T. Yanai and G. K. L. Chan, *J. Chem. Phys.*, 2008, **128**, 144117.

63 S. Sharma and G. K.-L. Chan, *J. Chem. Phys.*, 2012, **136**, 124121.

64 S. Guo, M. A. Watson, W. Hu, Q. Sun and G. K. L. Chan, *J. Chem. Theory Comput.*, 2016, **12**, 1583–1591.

65 J. Cioslowski, *Int. J. Quantum Chem.*, 1990, **S24**, 15–28.

66 M. Giese, M. Albrecht and K. Rissanen, *Chemical Reviews*, 2015, **115**, 8867–8895.

67 M. García-Revilla, P. L. A. Popelier, E. Francisco and Á. Martín Pendás, *J. Chem. Theory Comput.*, 2011, **7**, 1704–1711.

68 G. Merino, M. A. Menéndez-Rojas, H. I. Beltrán, C. Corminboeuf and T. Heine, *J. Am. Chem. Soc.*, 2004, **126**, 16160–16169.

69 Z. Cui, Y. Ding, J. L. Cabellos, E. Osorio, R. Islas, A. Restrepo and G. Merino, *Phys. Chem. Chem. Phys.*, 2015, **17**, 8769–8775.

70 M. S. M. Malischewski and K. Seppelt, *Angew. Chem. Int. Ed.*, 2016, **55**, 1–4.

71 J.-D. Chai and M. Head-Gordon, *Phys. Chem. Chem. Phys.*, 2008, **10**, 6615–6620.

72 S. M. Bachrach, *Computational Organic Chemistry*, Wiley, 2nd ed., New York, 2014.

73 H. S. Yu and D. G. Truhlar, *Angew. Chem. Int. Ed.*, 2016, **55**, 9004–9006.

74 E. R. Sayfutyarova, Q. Sun, G. K.-L. Chan and G. Knizia, *J. Chem. Theory Comput.*, 2017, **13**, 4063–4078.

Table of Contents Graphic